Some Remarks on Perspective Shape-from-Shading Models

Emiliano Cristiani[1], Maurizio Falcone[2], and Alessandra Seghini[2]

[1] Dipartimento di Metodi e Modelli Matematici per le Scienze Applicate,
Sapienza - Università di Roma
`cristiani@dmmm.uniroma1.it`
[2] Dipartimento di Matematica, Sapienza - Università di Roma
`{falcone,seghini}@mat.uniroma1.it`

Abstract. The Shape-from-Shading problem is a classical problem in image processing. Despite the huge amount of articles that deal with it, few real applications have been developed because the usual assumptions considered in the theory are too restrictive. Only recently two new PDE models have been proposed in order to include in the model the perspective deformation of the image, this allows to drop the unrealistic assumption requiring that the point of view is very far from the object. We compare these two models and present two semi-Lagrangian approximation schemes which can be applied to compute the solution. Moreover, we analyze the effect of various boundary conditions on the first order equations corresponding to the models. Some test problems on real and virtual images are presented.

1 Introduction

The Shape-from-Shading problem is a classical inverse problem in image processing. The goal is to reconstruct a three-dimensional object (the *shape*) from the brightness variation (the *shading*) in a greylevel photograph of that scene. In the classical model it is assumed that the surface $z = u(x)$, $x \in \Omega \subset \mathbb{R}^2$ is a graph. In order to characterize the solution of the problem several assumptions are needed, here are the most classical ones (see *e.g.* [3]):

H_1 - The image reflects the light uniformly, *i.e.* the albedo (ratio between energy reflected and energy captured) is constant.
H_2 - The material is Lambertian, *i.e.* the brightness function $I(x)$ is proportional to the scalar product $\eta(x) \cdot \omega(x)$ where $\eta(x)$ is the normal to the surface at the point $(x, z(x))$ and $\omega(x)$ is the direction of the light at the same point.
H_3 - The light source is unique and the rays of light which lighten the scene are parallel, *i.e.* $\omega(x)$ is constant.
H_4 - Multiple reflections are negligible.
H_5 - The aberrations of the objective are negligible.
H_6 - The distance between the scene and the objective is much larger than that between the objective and the CCD sensor.

H_7 - The perspective deformations are negligible.

H_8 - The scene is completely visible by the camera, *i.e.* there are not hidden regions.

Under those assumptions, if the light source is vertical the solution can be characterized in terms of an eikonal type equation

$$|\nabla u(x)| = q(x) \text{ for } x \in \Omega \quad \text{where} \quad q(x) = \sqrt{\frac{1 - I^2(x)}{I^2(x)}}. \tag{1}$$

Since the object can (obviously) have sharp sides there is no reason to assume that the solution of (1) is regular, the natural framework for this characterization is that of weak solutions in the viscosity sense (see *e.g.* [14,9]). However, the problem is not well-posed and suffers from the convex-concave ambiguity which makes impossible to prove uniqueness results without additional assumptions on the surface. A lot of work has been done to obtain uniqueness results in the framework of weak solution and new concepts have been introduced, such as that of maximal solutions (see [2] and references therein, [1,15] for some numerical applications and [8] for an up-to-date survey).

Recently, more realistic models have been proposed (see Prados and Faugeras [12], Tankus, Sochen and Yeshurun [16], Courteille, Crouzil, Durou and Gurdjos [4]). Since those papers, the Shape-from-Shading was finally applied to some real problems like reconstruction of faces ([11,13]), reconstruction of human organs ([17]) and the digitization of documents without scanners ([5,6,3]). We will examine in particular two models. The first, proposed in [4], drops the assumption H_7 so that it takes into account the perspective deformation due to the finite distance between the camera and the scene. In this model the distance of the light source is infinite so that all the rays are parallel (in the sequel this model will be denoted by $PSFS_\infty$). We perform a numerical approximation of the first order PDE related to the new problem via a semi-Lagrangian discretization and we discuss the effect of several possible boundary conditions for it.

In the second model, proposed by Prados and Faugeras [12], the assumptions H_3 and H_7 are dropped. The light source is placed at the optical center as in [10] so that this model is more realistic under flash lighting conditions (in the sequel this model will be denoted by $PSFS_r$). We present a semi-Lagrangian scheme also for this model.

The goal of this paper is to compare the two models and test them on real and synthetic images trying to sketch some conclusions which can be useful for future applications.

2   The $PSFS_\infty$ Problem

In this section we get rid of assumption H_7 so we will take into account the perspective deformation due to the fact that the camera is close to the scene.

Let us define the model adopting the same notations used in [5]. The point $O = (X_0, Y_0)$ is the principal point of the image, *i.e.* it is the intersection between
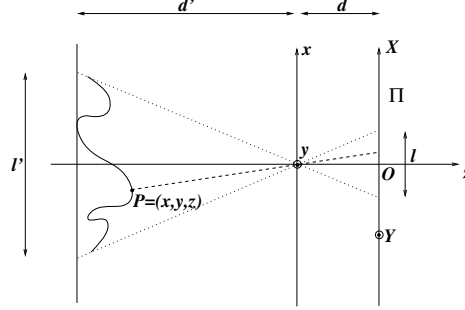
Fig. 1. The PSFS$_\infty$ model

the perspective plane Π and the z axis, d and d' are respectively the distance of the objective from the perspective plane (the CCD sensor) and the distance of the objective from the (flat) background, l and $l' = \frac{d'}{d}l$ are respectively the length of a generic segment in the perspective plane and the length of the real segment corresponding to it (see Figure 1 and [5] for more details). The representation of a point P on the surface in terms of the (X, Y) coordinates of a point in the perspective plane Π is given by three parametric equations

$$x = r(X, Y), \; y = s(X, Y), \; z = t(X, Y) \tag{2}$$

where (see [5])

$$\begin{cases} r(X,Y) = \frac{X - X_0}{d} t(X,Y) \\ s(X,Y) = \frac{Y - Y_0}{d} t(X,Y). \end{cases} \tag{3}$$

Then the problem amounts to compute the third component t. This is the most difficult task since t is the solution of the following eikonal type equation

$$\left(\frac{d}{\bar{t}(X,Y)} \right)^2 |\nabla t(X,Y)|^2 = \frac{I_{max}^2}{I'(X,Y)^2} - 1 \quad \text{in } \Omega \tag{4}$$

where Ω is the internal region bounded by the silhouette of the object ($\partial \Omega$ will denote its boundary) which is embedded in a rectangular domain Q,

$$\bar{t}(X,Y) = t(X,Y) + (X - X_0, Y - Y_0) \cdot \nabla t(X,Y), \tag{5}$$

$$I'(X,Y) = \frac{I(X,Y)\left((X - X_0)^2 + (Y - Y_0)^2 + d^2\right)^2}{d^4}, \tag{6}$$

and I_{max} is a constant depending on parameters of the problem. The set $Q \setminus \Omega$ is the background.

Defining

$$f(X,Y) := \frac{1}{d^2} \left(\frac{I_{max}^2}{I'(X,Y)^2} - 1 \right) \tag{7}$$

we can write (4) as

$$|\nabla t(X,Y)| = \sqrt{f(X,Y)}\,|\bar{t}(X,Y)|. \tag{8}$$

We want to write (8) in a fixed point form and construct an approximation scheme for this equation. To this end it is important to note that $\bar{t}$ has a sign. In fact, the exterior normal to the original surface at the point P is given by $\hat{n}(P) = N(P)/|N(P)|$ where

$$N(P) := (d\,t_X(X,Y), d\,t_Y(X,Y), -\bar{t}(X,Y)) \tag{9}$$

and since $-\bar{t}$ must be positive (according to the orientation of the z axis in Figure 1), $\bar{t}$ must be negative. This implies that (8) is in fact

$$|\nabla t(X,Y)| + \sqrt{f(X,Y)}\big((t(X,Y) + (X - X_0, Y - Y_0) \cdot \nabla t(X,Y)\big) = 0. \tag{10}$$

Equation (10) must be complemented with some boundary conditions, typically we will consider the Dirichlet boundary condition

$$t = g(X,Y) \quad \text{on } \partial\Omega, \quad \text{where } -d' \leq g \leq 0. \tag{11}$$

We will come back later on to this point.

The standard semi-Lagrangian scheme for (10)-(11) is

$$t(X,Y) = F[t](X,Y) := \frac{1}{1+h}\inf_{a \in B(0,1)}\{t\,(b_h(X,Y,a))\} \qquad \text{in } \Omega \tag{12}$$

where

$$b_h(X,Y,a) = (X,Y) + h\left(\frac{-a}{\sqrt{f}} - (X,Y)\right) \qquad (X,Y) \in \Omega,\ a \in B(0,1) \tag{13}$$

and $B(0,1)$ is the unit ball in $\mathbb{R}^2$. Let us examine the properties of the F operator in order to guarantee convergence for the fixed point iteration. First, let us introduce the space $W = \{w : \Omega \to \mathbb{R}, \text{ such that } w|_{\partial\Omega} = g\}$.

Lemma 1. *[7] Under the above assumptions, the following properties hold true:*
a) F is a contraction mapping in $L^\infty(\Omega)$;
b) F is monotone, i.e. $s \leq t$ implies $F[s] \leq F[t]$;
c) Let $V = \{w \in W : -d' \leq w(X,Y) \leq 0\}$, then $F : V \to V$;

In practice, a variable step discretization h can be applied to obtain more accurate results depending on X, Y and a in such a way that

$$h(X,Y,a)\left(\frac{-a}{\sqrt{f}} - (X,Y)\right) = \Delta x \quad \text{for all } X,Y,a$$

where Δx is the space step discretization. Note that h should be interpreted as a time step used to integrate along characteristics in the semi-Lagrangian scheme. This trick reduces the number of iterations needed to reach convergence.

Now let us examine the algorithm. Lemma 1 guarantees that, starting from any initial guess $t^{(0)}$ which satisfies the boundary conditions, the fixed point iteration

$$t^{(n+1)} = F[t^{(n)}] \tag{14}$$

converges to the unique solution t^* (fixed point). The iterative algorithm stops when $\|t^{(n+1)} - t^{(n)}\|_\infty < \varepsilon$, where ε is a given tolerance.

We note that a direct consequence of the above Lemma is that one can obtain a monotone increasing convergence just starting from any function below the final solution, *e.g.* choosing $t^{(0)} \equiv -d'$ in the internal nodes and imposing the Dirichlet boundary condition $t^{(0)} = g(X, Y)$ on $\partial\Omega$. Moreover, property b) guarantees that $\bar{t} < 0$ for all $(X, Y) \in \Omega$ *at every iteration*, so the equation associated to the problem is always (10).

3   The PSFS$_r$ Model

This model gets rid of assumptions H$_7$ and H$_3$. It takes into account the perspective deformation *and* the closeness of the light source which is now located at the optical center.

Let us define the model adopting the same notations used in [13]. Let Ω be an open set of $\mathbb{R}^2$. Ω represents the image domain. We denote by $f > 0$ the focal length and by P a generic point on the surface. There exists a function $u : \Omega \to \mathbb{R}$ such that (see Fig. 2)

$$P = P(x, y) = u(x, y) m' \tag{15}$$

where

$$m' = \frac{f}{\sqrt{x^2 + y^2 + f^2}}\, m \quad \text{and} \quad m = (x, y, -f). \tag{16}$$

We also denote by $r(x, y)$ the distance between the light source and the point $P(x, y)$ on the surface. Note that $u(x, y) = \frac{r(x,y)}{f}$.

In [13] it was proved that $v = \ln(u)$ (u is strictly positive since we assume that the scene is placed in front of the optical center) is the solution of the following equation

$$-e^{-2v(x,y)} + \sup_{a \in B(0,1)} \{-b(x, y, a) \cdot \nabla v(x, y) - l(x, y, a)\} = 0, \quad (x, y) \in \Omega \tag{17}$$

once we define

$$l(x, y, a) := -I(x, y) f^2 \sqrt{1 - |a|^2}\,, b(x, y, a) := -J(x, y) R^T(x, y)\, D(x, y)\, R(x, y)\, a\,,$$

$$D(x, y) := \begin{pmatrix} f & 0 \\ 0 & \sqrt{f^2 + x^2 + y^2} \end{pmatrix}, \qquad R(x, y) := \frac{1}{(x^2 + y^2)^{1/2}} \begin{pmatrix} y & -x \\ x & y \end{pmatrix},$$

$$J(x, y) := I(x, y) f \sqrt{x^2 + y^2 + f^2}$$

where R^T is the transpose of the matrix R. Note that $l(x, y, a) = 0$ on $\partial B(0, 1)$, therefore in the numerical approximation we can not search only on $\partial B(0, 1)$ but we have to discretize the unit ball entirely. We have the following
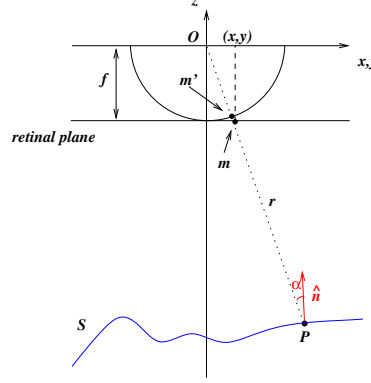
Fig. 2. The PSFS$_r$ model

Theorem 1. *Let Ω be bounded and smooth. If I is differentiable and if there exist $\delta > 0$ and M verifying $I \geq \delta$ and $|\nabla I| \leq M$, then equation (17) complemented with Dirichlet boundary condition $u = \phi$ on $\partial\Omega$ has a unique viscosity solution.*

Theorem 2. *Under the assumptions of Theorem 1, equation (17) complemented with state constraints boundary condition on $\partial\Omega$ has a unique viscosity solution.*

The proof of Theorems 1-2 can be found in [13]. These uniqueness results show that, under certain assumptions, the PSFS$_r$ model is well-posed. As we will see in the numerical experiments, the application of state constraint boundary condition (which is more convenient than Dirichlet's or Neumann's since it does not require a previous knowledge of any data) is typical of the PSFS$_r$ model due to its particular brightness attenuation and cannot be exported to the PSFS$_\infty$ model.

We present a semi-Lagrangian discretization for equation (17) which is simpler than that presented in [13] and which has a built-in up-wind correction. By standard arguments, we get, for $(x, y) \in \Omega$,

$$- v_h(x, y) + \inf_{a \in B(0,1)} \left\{ v_h((x, y) + hb(x, y, a)) + hl(x, y, a) \right\} + he^{-2v_h(x,y)} = 0.$$
(18)

We want to solve equation (18) following a fixed point method. Note that once we compute the control a^* where the infimum is attained we need some extra work to compute $v_h(x, y)$. In fact, let us define

$$c := v_h((x, y) + hb(x, y, a^*)) + hl(x, y, a^*)$$

and $t := v_h(x, y)$ for any (x, y) fixed. At every iteration we have to solve the equation

$$g(t) := -t + c + he^{-2t} = 0.$$

This additional problem is solved by applying Newton's method as in [13] (note that $g'(t) < 0$ for all $t \in \mathbb{R}$).

We start from any supersolution $v_h^{(0)}$ of (18) and we compute its solution, iterating the procedure until $\|v_n^{(n+1)} - v_h^{(n)}\|_\infty < \varepsilon$, where ε is a given tolerance. We choose the time step $h = h(x,y)$ in such a way $|h(x,y)b(x,y,a^*)| \le \Delta x$ and we discretize the unit ball $B(0,1)$ by means of ($\#directions \times \#circles$) points plus the central point.

The Effect of Boundary Conditions

As we have seen both models leads to a first order PDE which has to be complemented with a boundary condition in order to select a unique solution and run the approximation scheme. However, in practical applications boundary conditions on the surface are seldom known, so it useful to analyse in more detail the effect of different types of boundary conditions on the solution in order to define a minimal set of conditions which will allow to compute the exact solution.

In this section, we will briefly analyse the effect of Dirichlet, Neumann and state constraints boundary conditions on subsets of the boundary. Let us note first that boundary conditions should be imposed in a weak sense. The typical condition which defines a viscosity subsolution u of an equation of the form $H(x, u, \nabla u) = 0$, $x \in \Omega$ requires that for any test function $\varphi \in C^1(\overline{\Omega})$ and $x_0 \in \partial\Omega$ local maximum point for $u - \varphi$

$$\min\{H(x_0, u(x_0), D\varphi(x_0)), B(x_0, u(x_0), D\varphi(x_0))\} \le 0 \qquad (19)$$

where the function B is the operator describing the boundary conditions, *f.e.* $B(x, u, Du) = u - g$ for the Dirichlet condition. Similarly, the boundary condition for supersolutions requires that for any test function $\varphi \in C^1(\overline{\Omega})$ and $x_1 \in \partial\Omega$ local minimum point for $u - \varphi$

$$\max\{H(x_1, u(x_1), D\varphi(x_1)), B(x_1, u(x_1), D\varphi(x_1))\} \ge 0. \qquad (20)$$

The effect of the Dirichlet condition is to impose a value on u according to the above conditions, in particular the value $u(x) = g(x)$ is set at every point where $H(x, u(x), D\varphi(x)) \ge 0$ (for subsolutions) and $H(x, u(x), D\varphi(x)) \le 0$ (for supersolutions). Neumann boundary condition corresponds to the operator $B(x, u, Du) = \partial u / \partial n(x) - m(x)$ where $n(\cdot)$ represents the outward normal to the domain Ω. A typical use of it is when we know (or we presume) that the level curves of the surface are orthogonal to the boundary $\partial\Omega$ or to a subset of it where we simply choose $m(x) = 0$. The state constraints boundary condition is different from the above conditions since we do not impose neither a value for u nor a value for its normal derivative $\partial u / \partial n(x)$ (cfr. [1]). In this respect it has been interpreted as a "no boundary condition" choice although this interpretation is rather sloppy. In fact, a real function u bounded and uniformly continuous is said to be a *state constraints* viscosity solution if and only if it is a subsolution (in the viscosity sense) in Ω and a supersolution in $\overline{\Omega}$ (*i.e.* up to the boundary). It can be also stated as a Dirichlet boundary condition simply setting $g = C_g = constant$ provided $C_g > \max\limits_{x \in \Omega} u(x)$.

4   Numerical Experiments

We will show some tests for the two schemes implemented in MATLAB v.7, compare the two methods and try to draw some conclusions.

Numerical Experiments for PSFS$_\infty$
We choose the following parameters: $X_0 = 0$, $Y_0 = 0$, $d = 1$, $d' = 4$, $l = 0.75$ and $l' = 3$. The computational procedure follows the steps described in the previous sections. We choose 16 controls for the discretization of the unit ball $B(0,1)$ (all of them are placed on the boundary $\partial B(0,1)$).

Test 1: tent upside down
In this test we consider a ridge tent upside down and its photograph (see Fig. 3). We choose 121×121 pixels grid and we solve the equation imposing Dirichlet boundary condition on the silhouette of the tent.
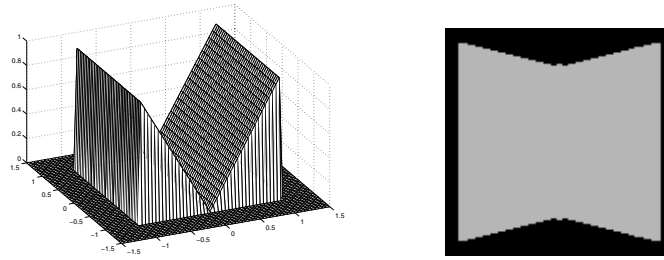

Fig. 3. Initial surface (left) and its photograph (right)

As we can see in Fig. 4, the reconstruction fails since the algorithm tries to compute the maximal solution instead of the correct solution. However, the shape of the domain (distorted in the photograph) is correctly straightened. Note that in Fig. 4-left MATLAB connects all points of the surface despite there is a hole in the domain of the reconstructed surface due to the fact that not all the background is visible by the camera. In Fig. 4-right the same surface is plotted by a slightly different point of view without interpolation.

Test 2: Real image
In this test we used a real photograph where the effect of perspective is visible. The surface is a sheet of paper with the shape of a roof tile. For this image the parameter values are: $l = 6.91 \ mm$, $d = 5.8 \ mm$, $l' = 200 \ mm$, $d' = \frac{l'}{l} d = 167.87 \ mm$, $\Delta x = 0.05 \ mm$. We note that we performed the light correction (6) in the preprocessing step, so we can assume $I_{max} = 1$ during computation. Figure 5 shows the photograph (128×128 pixels) and the surface reconstructed using Dirichlet boundary condition only on the left and right sides of the boundary and state constraints elsewhere (top and bottom sides).
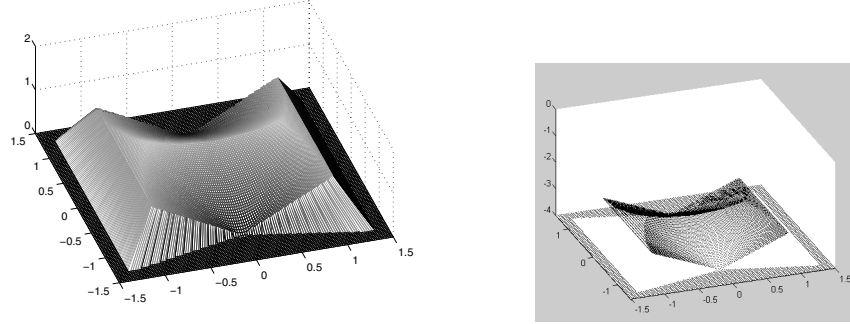
Fig. 4. Reconstructed surface with Dirichlet boundary condition. Interpolated (left) and non interpolated (right)
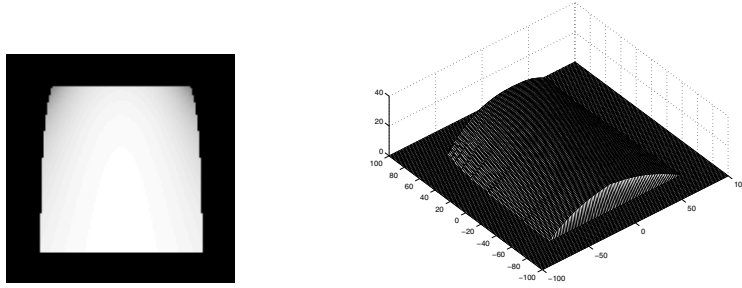

Fig. 5. The photograph, 128×128 pixels (left) and its reconstructed surface with mixed Dirichlet and state constraints boundary condition (right)

We can see that the solution is quite good considering the fact that light source (flash camera) is not far from the object and that direction of light source is not perfectly vertical as the mathematical model would have required.

We also tried to reconstruct the surface with two more practical boundary conditions. In the first case, we fixed a Dirichlet condition t^0 only on a vertical line in the center of the image (column 64) and then we turned over the computed surface with respect to the value t^0 (see Figure 6-left). Note that the solution is not very sensitive with respect to value t^0, so a rough knowledge of the behavior of the surface can be sufficient. We can see that the solution is quite good. We have a large maximum norm error on the boundary (17.7 mm, 41% of the maximum height of the tile), but not inside. In fact, assuming that the reconstructed surface in Figure 5-right is the exact solution, the average error on all nodes for Figure 6-left is about 1.2 mm.

In the second case (see Figure 6-right), we fixed a Dirichlet condition t^0 only on the point $(64, 64)$ (at the center of the image) and then we turned over the computed surface as before. Note that in this case the solution has a shape very
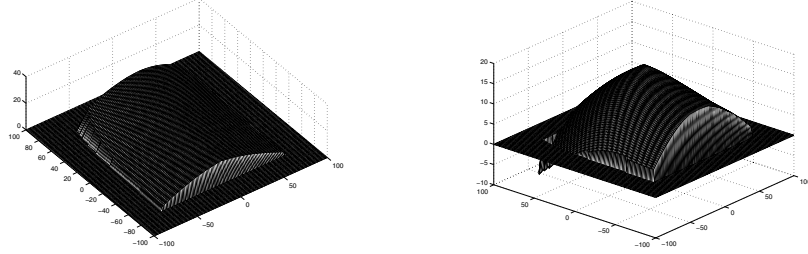
Fig. 6. Reconstructed surface with Dirichlet boundary condition on the center line (left) and on the center point (right, different scale)
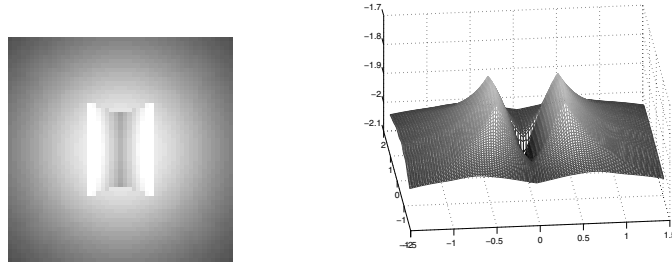

Fig. 7. The photograph (left) and its reconstructed surface with state constraints boundary condition (right)
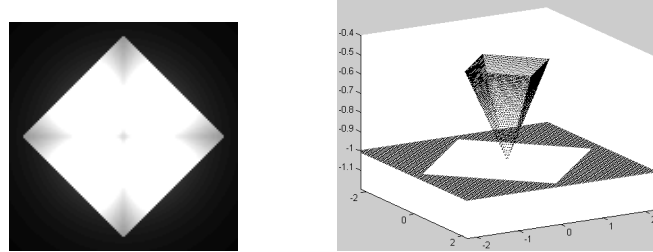

Fig. 8. The photograph (left) and its reconstructed surface with Dirichlet boundary condition (right)

different from the expected solution since it has a global maximum at the central point $(64, 64)$. In these three tests the iterative procedure converges respectively in 167, 185 and 190 iterations, with $\varepsilon = 10^{-6}$.

Numerical experiments for PSFS$_r$
Test 3: tent upside down
In this test we consider a ridge tent upside down as in Test 1. We use a 100×100

pixels initial image and we choose $f = 1$ and $16 \times 2 + 1$ controls. Convergence is reached in 159 iterations. In Fig. 7 we show the result obtained by the PSFS$_r$ algorithm imposing state constraints boundary condition on the boundary of the square (*i.e.* the background). In this case the reconstruction is definitively better than the previous one, considering that any boundary data was needed. On the other hand, we observe that the hole in the domain due to the regions in full shade is not reconstructed properly. In fact, the surfaces connecting the tent and the background are really computed and they are not due to the MATLAB's interpolation.

Test 4: pyramid upside down
In the second test we consider a pyramid upside down with the vertex standing on a flat background. We use a 128×128 pixels initial image and we choose $f = 1/4$. We impose Dirichlet boundary condition on the boundary of the pyramid (so we do not compute on the background). The initial image and the reconstructed surface are shown in Fig. 8. In this case we obtain a perfect result.

5   Conclusions

The above discussion allow us to draw some partial conclusions:

1. The PSFS$_r$ is a more realistic model under flash lighting conditions. It allows to compute a solution without a previous knowledge of the surface just applying state constraints boundary conditions. However, this model has a more delicate initialization and the corresponding algorithm does not converge for any initial guess.
2. The PSFS$_\infty$ requires additional information on the boundary (state constraints will not work in every situation). The algorithm is simpler and will converge starting from any initial guess.
3. The computational cost related to PSFS$_r$ is higher since it requires a Newton iteration for every fixed point iteration.

References

1. Camilli, F., Falcone, M.: Approximation of optimal control problems with state constraints: estimates and applications. B. S. Mordukhovic, H. J. Sussman (editors), "Nonsmooth analysis and geometric methods in deterministic optimal control", IMA Volumes in Applied Mathematics **78**, 23-57, Springer Verlag, 1996.
2. Camilli, F., Siconolfi, A.: Discontinuous solutions of a Hamilton-Jacobi equation with infinite speed of propagation. SIAM Journal on Mathematical Analysis, **28** (1997), 1420-1445.
3. Courteille, F.: Vision monoculaire: contributions théoriques et application à la numérisation des documents. Ph.D. thesis, Université Paul Sabatier, Toulouse, France, 2006.
4. Courteille, F., Crouzil, A., Durou, J.-D., Gurdjos, P.: Shape from shading en conditions réalistes d'acquisition photographique. Actes du $14^{\text{ème}}$ Congrès Francophone de Reconnaissance des Formes et Intelligence Artificielle (volume II), 925-934, Toulouse, France, 2004.

5. Courteille, F., Crouzil, A., Durou, J.-D., Gurdjos, P.: Towards shape from shading under realistic photographic conditions. Proceedings of the 17th International Conference on Pattern Recognition (volume II), 277-280, Cambridge, England, 2004.

6. Courteille, F., Crouzil, A., Durou, J.-D., Gurdjos, P.: Shape from shading for the digitization of curved documents. Machine Vision and Applications, 2006 (to appear).

7. Cristiani, E., Falcone, M., Seghini, A.: Numerical solution of the perspective Shape from Shading problem. Proceedings of "Control Systems: Theory, Numerics and Applications" PoS (CSTNA2005) 008, `http://pos.sissa.it/`.

8. Durou, J.-D., Falcone, M., Sagona, M.: A survey of numerical methods for Shape from Shading. Rapport IRIT 2004-2-R, Université Paul Sabatier, Toulouse, France, 2004. Submitted to Computer Vision and Image Understanding, under revision.

9. Lions, P.-L., Rouy, E., Tourin, A.: Shape from shading, viscosity solution and edges. Numerische Mathematik, **64** (1993), 323-353.

10. Okatani, T., Deguchi, K.: Reconstructing Shape from Shading with a Point Light Source at the Projection Center: Shape Reconstruction from an Endoscope Image. Proceedings of the 13th International Conference on Pattern Recognition (volume I), Vienna, Austria, 1996, 830-834.

11. Prados, E.: Application of the theory of the viscosity solutions to the Shape From Shading problem. Ph.D. thesis, Univ. of Nice - Sophia Antipolis, France, 2004.

12. Prados, E., Faugeras, O.: "Perspective Shape from Shading" and viscosity solutions. Proceedings of the 9th IEEE International Conference on Computer Vision (volume II), 826-831, Nice, France, 2003.

13. Prados, E., Faugeras, O., Camilli, F.: Shape from Shading: a well-posed problem?. Rapport de Recherche n. 5297. INRIA Sophia Antipolis, 2004.

14. Rouy, E., Tourin, A.: A viscosity solutions approach to Shape-from-Shading. SIAM J. Numer. Anal., **29** (1992), 867-884.

15. Sagona, M.: Numerical methods for degenerate eikonal type equation and applications. Ph.D. thesis, Dipartimento di Matematica, Università di Napoli "Federico II", Italy, 2001.

16. Tankus, A., Sochen, N., Yeshurun, Y.: A new perspective [on] Shape-from-Shading. Proceedings of the 9th IEEE International Conference on Computer Vision (volume II), 862-869, Nice, France, 2003.

17. Tankus, A., Sochen, N., Yeshurun, Y.: Reconstruction of medical images by perspective Shape-from-Shading. Proceedings of the 17th International Conference on Pattern Recognition (volume III), 778-781, Cambridge, England, 2004.